ENERGY AND ENERGY SPREAD MEASUREMENTS USING THE RUTHERFORD SCATTERING TECHNIQUE FOR TUNING THE SARAF SUPERCONDUCTING LINAC

J. Rodnizki#, A. Perry, L. Weissman Soreq NRC, Yavne 81800, Israel

Abstract

The SARAF Phase-I accelerator consists of an ECR ion source (20 keV/u), 4-rod RFQ (1.5 MeV/u) and a superconducting module housing 6 half-wave resonators and 3 superconducting solenoids (4-5 MeV). The ions energy and energy spread were measured using the Rutherford scattering technique. This technique is used to tune the cavities to the desired amplitude and phase. The downstream HWR is used as a buncher and the beam energy spread as function of the bunching RF voltage is applied to estimate the longitudinal emittance. In this work, we present a longitudinal emittance measurement algorithm, based on the bunch energy spread as a function of the buncher's amplitude. The tuning and measured longitudinal parameters are in qualitative agreement with the predicted beam dynamics simulation.

INTRODUCTION

SARAF (Soreq Applied Research Accelerator Facility) is currently under construction at Soreq NRC. It will consist of up to 40 MeV high current (up to 4 mA) CW, 176MHz RF superconducting linac of protons and deuterons. The linac status and technical description of its components are given in [1,2]. Phase one of the SARAF linac includes a 20 keV/u proton/deuteron ECR ion source, LEBT, 1.5MeV/u four rods RFQ and a Prototype Superconducting Module (PSM) with six $\beta = 0.09$ HWRs.

In this work we present a method to evaluate the longitudinal emittance at the RFQ exit and along the PSM, based on the measurements of the bunch energy distribution via a silicon detector which is part of a Rutherford scattering halo monitor [3], which is placed within a diagnostic plate (D-Plate) downstream of the PSM. The presented algorithm is similar to the one using a set of measurements of the temporal distribution of the bunch as a function of a downstream diagnostic cavity voltage [4, 5, 6].

LONGITUDINAL EMITTANCE EXTRACTION ALGORITHM

The longitudinal emittance measurement process is defined by three transfer matrixes: a drift matrix from the point where the longitudinal emittance is measured to the diagnostic cavity, an acceleration matrix, the diagnostic cavity, with energy gain *Uacc* which parameters are varied and used for the evaluation and another drift matrix from the (middle) of the diagnostic cavity to the halo-monitor. The diagnostic element length in the matrix is zero. Algebraically, particle phase and energy with respect to the synchronous particle phase and energy at the halo monitor ($\Delta\phi_x$, ΔE_x) are generated by the matrix element R as function of the diagnostic cavity variables (U_{acc}, ϕ) and from the point-of-measurement values ($\Delta\Phi_e$, ΔE_e) by:

$$\begin{bmatrix}\Delta\phi_x\\ \Delta E_x\end{bmatrix} = R*\begin{bmatrix}\Delta\phi_e\\ \Delta E_e\end{bmatrix};\quad R=\begin{bmatrix}1 & Y_2\\ 0 & 1\end{bmatrix}\begin{bmatrix}1 & 0\\ X & 1\end{bmatrix}\begin{bmatrix}1 & Y_1\\ 0 & 1\end{bmatrix} \quad (1)$$

X and Y_i are given by:

$$X = -Uacc * \sin(\phi/360 * 2\pi) * 2\pi/360$$
$$Y_i = -((360/T)*(D_i/\beta c))/(mc^2\gamma_i^3\beta_i^2)$$

Where ϕ is the synchronous acceleration phase, T is the beam period (T=1/f, f=176 MHz), m is the particle mass and D_i are the relevant drift distances.

The development of the particle energy with respect to the synchronous particle energy along an acceleration element is given by:

$$\delta\Delta E = -Uacc*\sin(\phi/360*2\pi)*2\pi/360*\Delta\phi = X*\Delta\phi$$

Where $\Delta\phi$ is the particle phase with respect to the synchronous particle acceleration phase ϕ, and *Uacc* is the HWR energy gain. The development of the particle phase with respect to the synchronous phase along a drift element D is given by:

$$\delta\Delta\phi = -360/T*D/(\beta c)*\Delta E/(mc^2\gamma^3\beta^2) = Y*\Delta E$$

Where ΔE is the particle energy with respect to the synchronous particle energy: $\Delta E/(mc^2\gamma^3\beta^2) = \Delta\beta/\beta$

The beam matrix σ_x at the halo monitor is given by:

$$\begin{bmatrix}\sigma_{55x} & \sigma_{56x}\\ \sigma_{65x} & \sigma_{66x}\end{bmatrix} = R*\begin{bmatrix}\sigma_{55e} & \sigma_{56e}\\ \sigma_{65e} & \sigma_{66e}\end{bmatrix}R_T$$

The matrix R is defined in Eq. 1 and σ_e is the beam matrix at the measurement point. The explicit σ_x terms are:

$$\sigma_{55x} = \sigma_{55e}(1+XY_2)^2 + 2\sigma_{56e}(1+XY_2)(Y_1+XY_1Y_2+Y_2) + \sigma_{66e}(Y_1+XY_1Y_2+Y_2)^2$$
$$\sigma_{56x} = \sigma_{55e}(1+XY_2)X + \sigma_{56e}((Y_1+X_1Y_1Y_2+Y_2)X + (1+XY_2)(1+XY_1)) + \sigma_{66e}(Y_1+XY_1Y_2+Y_2)(1+XY_1)$$
$$\sigma_{66x} = \sigma_{55e}(X^2) + 2\sigma_{56e}(X+X^2Y_1) + \sigma_{66e}(1+XY_1)^2$$

In order to clearly apply the method, we express the measured energy variance at the halo monitor, σ_{66x}, as a function of X, the energy gain per degree:

$$\sigma_{66x}(X) = (\sigma_{55e}+2Y_1\sigma_{56e}+Y_1^2\sigma_{66e})X^2 + 2(\sigma_{56e}+Y_1\sigma_{66e})X + \sigma_{66e} = p_1X^2+p_2X+p_3 \quad (2)$$

#Jacob.Rodnizki@gmail.com

The beam matrix elements at the measurement point σ_e are:

$$\sigma_{66e} = p_3; \sigma_{56e} = p_2/2 - Y_1\sigma_{66e}; \sigma_{55e} = p_1 - 2Y_1\sigma_{56e} - Y_1^2\sigma_{66e}$$

The resulting longitudinal beam matrix σ_e parameters are:

$$\varepsilon = \sqrt{(\sigma_{55e} * \sigma_{66e} - \sigma_{56e} * \sigma_{56e})}$$

$$\hat{\beta} = \sigma_{55e}/\varepsilon, \quad \hat{\alpha} = -\sigma_{56e}/\varepsilon$$

$$\sigma_e = \varepsilon \begin{bmatrix} \hat{\beta} & -\hat{\alpha} \\ -\hat{\alpha} & \hat{\gamma} \end{bmatrix}$$

MEASUREMENTS

The Algorithm was applied to evaluate the longitudinal emittance of proton and deuteron beams at SARAF.

Proton Beam Measurements, Case 1

A 0.24 mA 3.7 MeV proton beam was accelerated through the 6 cavities of the PSM and measured at the D-plate, based on beam dynamics simulations with TRACK [7] . Then the longitudinal emittance was evaluated at cavity 3 exit (2.0 MeV) while cavity 4 and 5 were detuned. The rms longitudinal emmitance was found by variation of the synchronous phase at cavity 6. The emittance extracted from the energy variance at the D-plate halo monitor as function of the cavity accelerating voltage per degree for each synchronous phase is 120±5π deg-keV [8].

The evaluated longitudinal emittance, 120±5 π·deg·keV, was higher than the RFQ exit result 30 π deg-keV reported in Ref. 9, which was based on fast Faraday cup measurements. The source of the discrepancy is as follows: the fast Faraday cup temporal bunch measurements [9] were recorded within the nominal RFQ power time interval along the pulse. However, the halo-monitor measurements were continuous, so they included the large emittance part of the beam, due to the RFQ power rise time (we plane to limit the silicon detector measurements to the pulse plateau zone). In addition, the measurements in this work are conducted with a low instantaneous current proton beam 0.24 mA 1Hz 100μs 0.01%DC. Therefore, the space charge effect that reduced the longitudinal emittance growth along the RFQ in the temporal 3mA measurement is not significant here.

The setup in this work affects the emittance growth measurement by: (1) The voltage in the diagnostic cavity was constant and the phase was changed, varying both the beam's energy and energetic width. A more come way would be to set the cavity to a bunching phase and change its voltage, which in turn changes the energetic width without changing the synchronous beam energy. (2) Cavity 4 and 5 were detuned and act as a long drift towards the diagnostic element cavity 6. As a result the bunch was longitudinally spread at the diagnostic cavity and affected the beam emittance.

Proton Beam Measurements, Case 2

A modified beam dynamics setup was adopted to overcome the above limitations (1-2). The design was optimized for minimal emittance growth along the PSM based on the available accelerating voltage at each cavity rather than for maximum beam energy at the PSM exit (see table 1). The longitudinal emittance at the exit of cavity 4 was evaluated. The synchronous phase of cavity 4 (-35 degrees) enhances longitudinal bunch convergence towards the diagnostic element cavity 6 while cavity 5 was detuned. Cavity 6 was operated as a buncher at -95 degrees synchronous phase. The energy variance at the halo monitor was measured as a function of cavity 6 acceleration voltage from 53-530 keV. The longitudinal emittance was obtained by fitting the measured energy variance to a quadratic polynomial as function of the applied energy gain per degree, see Figs. 1,2.

Table 1: Accelerating Voltages and Synchronous Phases for the 3.16 MeV Proton Beam Run

Cavity	Acceleration voltage [kV]	Energy [MeV]	Synchronous Phase [deg]
1	150	1.50	-95
2	0	1.50	0
3	593	1.93	0
4	500	2.28	-35
5	500	2.68	-30
6	500	3.16	0

The extracted rms longitudinal emittance value is now 90 πdeg-keV. The beam dynamics simulation value for a low current proton beam is 60 πdeg-keV. The present measured result is in better agreement with the beam dynamics simulation value than the 120 πdeg-keV measured at the test setup reported in [8].

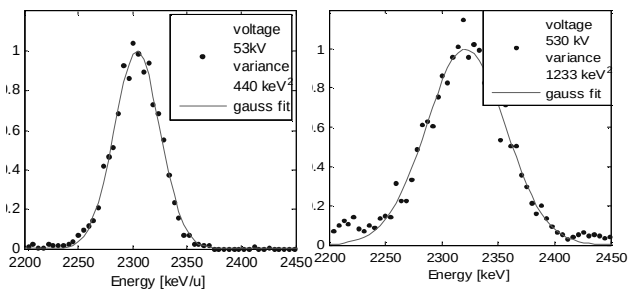

Figure 1: The proton beam measured energy distribution for different cavity applied voltages.

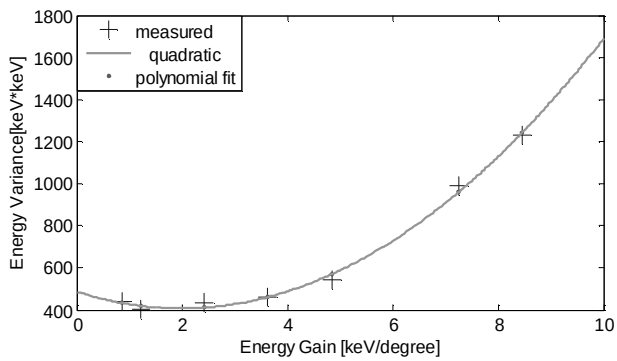

Figure 2: The proton beam measured energy variance (Eq. 2) versus the energy gain per degree in the diagnostic cavity.

Deuteron Beam Measurements

The algorithm was applied at a low current 0.4 mA deuteron beam for a qualitative longitudinal emittance evaluation at the RFQ exit as function of the RFQ power. Cavity 1 was used as a diagnostic cavity at -90 degrees buncher synchronous phase, while the cavity voltage was varied during the longitudinal evaluation measurements. Cavities 2-6 were detuned. Then the RFQ power 237kW that generated the lowest emittance was adopted for the PSM test, see table 2. This power is in reasonable agreement with the 61.5 kW RFQ power applied for the proton beam measurements. A similar minimum of the longitudinal emittance as function of the RFQ power at 61.5 kW was found using the fast-Faraday-cups during the proton beam operation [8].

Table 2: The Evaluated RFQ Longitudinal Emittance at the 0.4 mA Deuteron Beam Test

RFQ Power [kW]	Long. Emittance [pi deg keV/u]	Alpha	Beta [deg/(keV/u)]
227	261	-1.8	3.50
237	207	-1.25	1.92
249	367	-0.45	1.36

The RFQ power that generated the lowest emittance was adopted for the PSM beam test. The cavities acceleration voltages and synchronous phases for deuterons accelerated in the PSM are given in table 3. Then, the deuteron longitudinal emittance was measured at the exit of cavity 4 while cavity 5 was detuned and cavity 6 served as a diagnostic cavity with varying accelerating voltage at -90 degrees synchronous phase. The polynomial fit of the energy variance as function of the diagnostic cavity voltage is shown in Figure 3. The yielded longitudinal emittance at the deuteron beam PSM test is presented in table 4. The expected emittance for higher current (2 mA) is lower than the current evaluated value.

Table 3: Accelerating Voltages and Synchronous Phases for the 0.4 mA Deuteron Beam Test

Cavity	Acceleration voltage [kV]	Energy [MeV/u]	Synchronous Phase [deg]
1	288	1.50	-95
2	0	1.50	0
3	593	1.70	0
4	500	1.86	-35
5	500	1.97	-60
6	500	2.17	0

Table 4: The evaluated longitudinal emittance at HWR 4 for the 0.4 mA deuteron beam test.

RFQ Power [kW]	Long. Emittance [pi deg keV/u]	Alpha	Beta [deg/(keV/u)]
HWR 4	233	-1.15	0.72

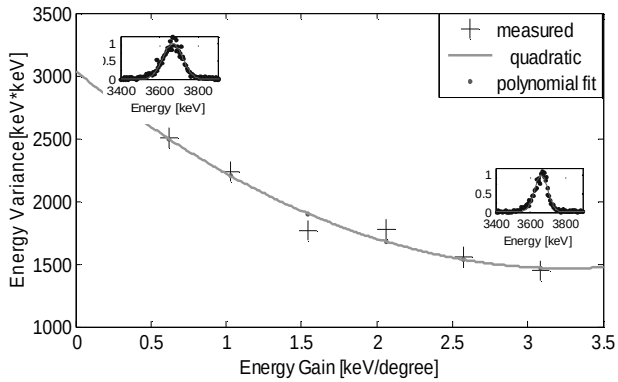

Figure 3: The deuteron beam measured energy variance versus the energy gain per degree in the diagnostic cavity.

CONCLUSION

The longitudinal emittance evaluation based on beam energy variance measurements seems to generate results, which are qualitatively consistent with simulated values. Possible sources of inconsistencies in the first measurements reported in this paper were discussed. Further benchmark measurements will take place in the near future in order to further evaluate this method.

REFERENCES

[1] L. Weissman et al., "SARAF Accelerator Commissioning Results and Phase II Construction Status", These Proceedings, WE102.

[2] A. Nagler et al., “Status of the SARAF Project”, LINAC'06, Knoxville, August 2006, MOP054, p. 168 (2006).

[3] L. Weisman, D. Berkovits, Y. Eisen, S. Halfon, I. Mardor, A. Perry, J. Rodnizki, K. Dunkel, C. Piel, D. Trompetter, P. vom Stein, “First Experience with Proton Beams Using the Rutherford Scattering Monitor”, DIPAC09, Basel (2009).

[4] P. N. Ostroumov, “Measurements of beam longitudinal parameters” ESS-Bilbao Workshop, March 17, 2009.

[5] Yu. V. Bylinsky, A. V. Feschenko, P. N. Ostroumov, “Longitudinal Emittance Measurement of the 100 MeV Proton Beam” PAC’91

[6] A. V. Feschenko et al., “Longitudinal Beam Parameters Study in the SNS Linac”, PAC07, Knoxville (2007).

[7] P. N. Ostroumov et al., "TRACK", ANL, March 2006.

[8] I. Mardor et al., "The SARAF CW 40 MeV Proton/Deuteron Accelerator", SRF'09, Berlin, MOODAU04 (2009).

[9] C. Piel et al., "Phase 1 Commissioning Status of the 40 MeV Proton/Deuteron Accelerator SARAF", EPAC'08, Geona, June 2008, THPP038, p. 3452.